THE ASTROPHYSICAL JOURNAL, 522:1088–1099, 1999 September 10

STOCHASTIC DYNAMICS OF FIELD GENERATION IN CONDUCTING FLUIDS

BRIAN F. FARRELL
Department for Earth and Planetary Sciences, Harvard University, Pierce Hall, 29 Oxford Street, Cambridge, MA 02138; farrell@io.harvard.edu
AND
PETROS J. IOANNOU
Division of Astronomy, Astrophysics, and Mechanics, Department of Physics, University of Athens, Panepistimiopolis, 15784 Zografos, Athens, Greece; pji@atlas.uoa.gr
Received 1998 July 20; accepted 1999 April 19

ABSTRACT

The large-scale magnetic fields of stellar and galactic bodies are generally understood to be organized and amplified by motions in the conducting fluid media of these bodies. This article examines a mechanism by which continual excitation of the conducting fluid by small-scale fields results in production of large-scale fields. The excitation of the induction equation by small-scale fields is parameterized as stochastic forcing, and the crucial role of the nonnormality of the induction operator in determining the spatial and temporal structure of variation in the large-scale fields is emphasized. A cylindrically symmetric helical flow is used to provide illustrative examples.

Subject headings: hydrodynamics — ISM: magnetic fields — MHD — Sun: magnetic fields

1. INTRODUCTION

It is generally accepted that the magnetic fields of stars and galaxies are amplified and organized by magnetohydrodynamic processes associated with motions in the conducting fluid of these bodies. This process of field amplification is governed by the induction equation for the magnetic field $\boldsymbol{B}$ in a conducting fluid medium with velocity $\boldsymbol{v}$, which can be written in the nondimensional form:

$$\frac{\partial \boldsymbol{B}}{\partial t} = \nabla \wedge (\boldsymbol{v} \wedge \boldsymbol{B}) + \frac{1}{R_m} \nabla^2 \boldsymbol{B} , \tag{1}$$

$$\nabla \cdot \boldsymbol{B} = 0 , \tag{2}$$

where representative dimensional scales for the spatial extent of the domain, L, and for the magnitude of the velocity of the mean motion, U, have been taken, and time has been nondimensionalized by L/U. The induction equation can be characterized by a single nondimensional number $R_m = UL/\eta$, the magnetic Reynolds number, where η is the magnetic diffusivity of the medium.

The induction equation governing the dynamics of magnetic fields in a moving fluid is explicitly linear in the magnetic field so that if the velocity field is known, the properties of the magnetic field can be obtained by linear methods. Boundary conditions on the magnetic field are usually chosen to correspond either to an idealized insulator, in which case $\boldsymbol{B}$ is continued into a potential field in the insulating region, or to a perfect conductor, in which case both the normal component of the magnetic field and the tangential component of the current are required to vanish.

The traditional procedure used to determine the stability of equation (1) is to assume modal solutions of the form $\boldsymbol{B} = \hat{\boldsymbol{B}} e^{\sigma t}$ so that equation (1) becomes an eigenproblem for the generally complex eigenvalue σ:

$$\sigma \boldsymbol{B} = \nabla \wedge (\boldsymbol{v} \wedge \boldsymbol{B}) + \frac{1}{R_m} \nabla^2 \boldsymbol{B} . \tag{3}$$

Exponential instability occurs for solutions $\boldsymbol{B}$ with Re $\sigma > 0$. Historically, demonstrating existence of an unstable eigenmode was important for establishing the possibility of field growth in light of the antidynamo result of Cowling (1934). For cases in which the induction equation has a complete set of orthogonal eigenfunctions, the eigenspectrum exhausts the possibilities for perturbation growth so that the boundary in R_m separating regions of Re $\sigma > 0$ from those with Re $\sigma < 0$ also separates regions in which all perturbations decay from regions in which at least one perturbation grows. In cases of physical interest, the induction equation does not in general have orthogonal eigenvectors, therefore there is the possibility of perturbation growth even in cases for which all eigenvalues of equation (3) have Re $\sigma < 0$.

Recently it has been more widely appreciated that concentrating on the modal solution form greatly restricts the dynamics of field growth allowed by equations (1) and (2). Recognition of the importance of nonmodal perturbation growth in fluid mechanics goes back to the work of Kelvin (1887) and Orr (1907), and nonmodal growth processes have been identified in connection with the formation of cyclones (Farrell 1982, 1984, 1989) and in the transition to turbulence (Farrell 1988; Gustavsson 1991; Butler & Farrell 1992; Reddy & Henningson 1993; Farrell & Ioannou 1993a). The possibility of nonmodal growth of magnetic field in the induction equation was discussed by Moffatt (1978) and more recently by Childress & Gilbert (1995).

The possibility of transient growth depends on the nonnormality of the operator. An operator is nonnormal if it does not commute with its adjoint in a chosen inner product. The inner product with most physical significance for our problem is the volume-integrated magnetic energy associated with the L_2 norm of the magnetic field $\boldsymbol{B}$. If the operator has a decaying spectrum, it can amplify perturbations only in norms associated with inner products for which it is nonnormal. Those initial perturbations that amplify and define the growing subspace of the operator and methods for identifying them in the context of the problem of magnetic field generation are presented in Farrell & Ioannou (1998).

In addition to providing methods for analyzing nonmodal growth of deterministic initial perturbations in

highly nonnormal systems such as the induction equation, nonnormal analysis also provides methods for analyzing field maintenance in the statistically steady state due to continual excitation of the mean operator arising from unresolved velocity and magnetic fields. Unresolved scale effects have been previously parameterized as stochastic excitation of the underlying mean dynamical operators in the astrophysical context (Hoyng 1987a, 1987b, 1988, 1993; Choudhuri 1992; Ossendrijver, Hoyng, & Schmitt 1996), in the geophysical turbulence of the midlatitude atmospheric jet (Farrell & Ioannou 1995), and in laboratory turbulence of shear flow (Farrell & Ioannou 1993b, 1998).

In the case of magnetic fields, parameterization of forcing of the mean field by unresolved scales has traditionally taken the form of the α effect according to which the unresolved scales produce a coherent field with the structure of the curl of the mean field itself (Parker 1955; Braginskii 1965a, 1965b; Steenbeck, Krause, & Rädler 1966; Hoyng 1992). Observations, however, show a rich variability of the magnetic field both in space and time (Rand & Kulkarni 1989; Minter & Spangler 1996), suggesting that accounting for the stochastic nature of the forcing of the mean field by the unresolved scales may be necessary for a more complete understanding of field generation and maintenance from internal magnetohydrodynamic processes. Alternatively, forcing of the mean field may arise from outside the manifold of the internal magnetohydrodynamic processes. Examples of this would be the dynamical effects of massive stars generating strong winds and sporadic supernovae, both of which produce distortions of the field and generate turbulence (McCray & Kafatos 1987; Zweibel & Heiles 1997). In these cases of externally imposed forcing a stochastic analysis of the response of the induction equation is necessary to understand the organization of the large-scale fields.

2. STOCHASTIC DYNAMICS OF THE INDUCTION EQUATION

After separation of velocity and magnetic fields into mean (resolved) and deviation (unresolved) components, $\boldsymbol{v} = \bar{\boldsymbol{v}} + \boldsymbol{v}'$ and $\boldsymbol{B} = \overline{\boldsymbol{B}} + \boldsymbol{B}'$, the mean (large-scale) field is seen to evolve according to equation (1) as

$$\frac{\partial \overline{\boldsymbol{B}}}{\partial t} - \nabla \wedge (\bar{\boldsymbol{v}} \wedge \overline{\boldsymbol{B}}) - \frac{1}{R_m} \nabla^2 \overline{\boldsymbol{B}} = \overline{\nabla \wedge (\boldsymbol{v}' \wedge \boldsymbol{B}')} \,. \qquad (4)$$

Traditionally the effect of unresolved velocity and magnetic fields has been modeled using mean field parameterization. The most common mean field parameterization of the induction equation is to replace the effects of the deviations from the mean contained in the term on the right-hand side of equation (4) with two modifications of the equation; first, an increase of diffusion over its value due to conductivity alone in order to take account of the enhancement of diffusivity caused by the turbulence and, second, introduction of a term proportional to the curl of the mean magnetic field. This parameterization is referred to as the α effect because the term in the curl of $\boldsymbol{B}$ is often written in the form $\nabla \wedge \alpha \overline{\boldsymbol{B}}$. The magnitude of α can be shown under certain conditions to be proportional to the helicity of the perturbation velocity field and, in particular, to vanish with the helicity (Steenbeck & Krause 1966). This parameterization of the unresolved scales by the α effect is useful but not completely comprehensive. Unresolved magnetic fields in turbulent flows may have substantial spatial and temporal fluctuations that produce contributions to the forcing term on the right-hand side of equation (4) not accounted for by the time-invariant α effect. It follows that a complete characterization of the mean field maintained by equation (4) must involve analyzing the response of equation (4) to spatially and temporally varying fields (Hoyng 1987b, 1988, 1993; Choudhuri 1992; Ossendrijver et al. 1996).

In the physical systems addressed in this study, there is a well-defined large-scale flow that is disturbed by spatially and temporally varying perturbations arising from smaller scale magnetic and velocity fields. We study the large-scale magnetic field maintained by the unresolved scales. The large-scale magnetic field of interest here can be traced primarily to coherent stretching by the large-scale velocity field, resulting in amplification of large-scale magnetic field perturbations. In order to isolate this mechanism, the fluctuating term on the right-hand side of equation (4) is replaced by a stochastic forcing δ correlated in time and with prescribed spatial correlation. The forcing arising from the interaction between $\boldsymbol{v}'$ and $\boldsymbol{B}'$ is more complex than the white-noise parameterization we use, but more exact specification of the properties of the stochastic forcing is deferred while attention is directed toward characterizing the response of the mean induction equation to generic forcing. One reason for deferring more precise characterization of the forcing is the expectation that only a relatively small subspace of disturbances will be found to amplify sufficiently to play a significant role in maintaining the large-scale field. That most disturbances do not amplify significantly restricts the relevant components of the forcing produced by the unresolved scales. Dissimilar forcings may produce similar responses provided only that the forcings similarly excite these relatively few components that are highly amplified.

Although the derivation of equation (4) is formally rigorous, the physical meaning of the mean magnetic field and of deviations from the mean may be variously interpreted (Moffatt 1978; Hoyng 1987b, 1992). To be concrete, we interpret the bar in equation (4) to be an azimuthal average, in which case equation (4) describes a forced equation for the axisymmetric magnetic field, with the assumption that interaction between the nonaxisymmetric fluctuations in the magnetic and velocity fields result in generation of axisymmetric magnetic field. We consider the fluctuating velocity and magnetic fields to be stochastic and approximate the last right-hand term in equation (4) by

$$\overline{\nabla \wedge (\boldsymbol{v}' \wedge \boldsymbol{B}')} = \boldsymbol{f}(\boldsymbol{r}, t) \,, \qquad (5)$$

where $\boldsymbol{f}$ gives the spatial and temporal structure of stochastic forcing while at the same time assuring that the forcing is nondivergent and that it meets appropriate boundary conditions. For simplicity we consider a generic stochastic process that is normally distributed and δ-correlated in time with zero mean.

The physical mechanism envisioned in this formulation is distinct from that envisioned in theories based on exponential modal instability of the induction equation (1). Modal instability is supposed to produce from an infinitesimal initial condition an exponentially growing magnetic field with the structure of the most unstable mode. This field eventually reaches finite amplitude and equilibrates in some manner the theory does not specify. In contrast, from the

point of view of equation (4), the finite-amplitude field is regarded as maintained in a statistically steady state by disturbances produced by interaction between the unresolved velocity and magnetic field components. For highly nonnormal mean operators, the field maintained by this forcing does not strongly depend on the structure of the forcing. The reason is that a nonnormal operator greatly amplifies a subspace of perturbations (distinct from the eigenmodes of the operator), and this subspace, which is referred to in the sequel as the growing subspace of the operator, dominates the structure of the maintained magnetic field energy resulting from any reasonably broadband forcing. So long as the forcing adequately excites these growing structures, the structure of the maintained energy will be primarily determined by these amplifying structures and will be insensitive to the details of the forcing. In addition, the temporal variability of the magnetic field is controlled by the associated time development of the same dominant growing perturbations.

3. STOCHASTIC DYNAMICS OF THE AXISYMMETRIC FIELD IN A HELICAL FLOW

3.1. *Formulation*

Consider the axisymmetric flow in a cylindrical domain with azimuthal (θ) velocity $U_\theta = r\Omega(r)$ depending only on radius (r) and axial (z) velocity field, $U_z(r)$ also depending only on radius, but with no radial flow. Stochastically forced axisymmetric magnetic field perturbations,

$$B_r = \hat{B}_r(t, r)e^{ikz}\,, \quad B_\theta = \hat{B}_\theta(t, r)e^{ikz}\,, \quad B_z = \hat{B}_z(t, r)e^{ikz}\,, \tag{6}$$

evolve in time according to the induction equation (4). In cylindrical coordinates this takes the form

$$\frac{d\hat{B}_r}{dt} = -ikU_z\hat{B}_r + \frac{1}{R_m}\boldsymbol{L}\hat{B}_r + f_r(r, t)\,, \tag{7}$$

$$\frac{d\hat{B}_\theta}{dt} = -ikU_z\hat{B}_\theta + r\frac{d\Omega}{dr}\hat{B}_r + \frac{1}{R_m}\boldsymbol{L}\hat{B}_\theta + f_\theta(r, t)\,, \tag{8}$$

$$\frac{d\hat{B}_z}{dt} = -ikU_z\hat{B}_z + \frac{dU_z}{dr}\hat{B}_r + \frac{1}{R_m}\left(\boldsymbol{L} + \frac{1}{r^2}\right)\hat{B}_z + f_z(r, t)\,, \tag{9}$$

in which appears the diffusion operator in cylindrical polar coordinates:

$$\boldsymbol{L} = \frac{1}{r}\frac{d}{dr}\left(r\frac{d}{dr}\right) - \frac{1}{r^2} - k^2\,. \tag{10}$$

We denote the stochastic forcing by $f_r(r, t)$, $f_\theta(r, t)$, and $f_z(r, t)$, which satisfy the boundary conditions. To ensure nondivergence of the magnetic field, the stochastic forcing is required to be divergenceless. With a divergenceless forcing, the radial and azimuthal magnetic field equations (7) and (8) can be solved independently because they decouple from the axial equation (9). The axial magnetic field can then be obtained from

$$\frac{1}{r}\frac{d(r\hat{B}_r)}{dr} + ik\hat{B}_z = 0\,, \tag{11}$$

which enforces for the axisymmetric case nondivergence of the magnetic field. We consequently consider only the radial and azimuthal equations (7) and (8) with arbitrary magnetic field forcing $f_r(r, t), f_\theta(r, t)$.

With the differential operators discretized on n points using central differences, evolution of the magnetic field obeys the matrix induction equation:

$$\frac{dB}{dt} = \boldsymbol{A}B + \boldsymbol{F}\xi(t)\,, \tag{12}$$

where $B = [\hat{B}_r, \hat{B}_\theta]^T$ is the $2n$ column vector with the first n columns corresponding to the values of $\hat{B}_r$ at each grid followed by the collocated values of $\hat{B}_\theta$.[1] The spatially continuous stochastic noise $\boldsymbol{f}$ in equation (5) is approximated by the discrete forcing $\boldsymbol{F}\xi(t)$. The spatial distribution of the forcing is provided by the matrix $\boldsymbol{F}$. Physically, each column of $\boldsymbol{F}$ corresponds to a given magnitude and spatial structure of the forcing magnetic field. Inclusion of $\boldsymbol{F}$ in the formulation allows restriction of the spatial structure of the forcing magnetic field. The vector ξ is taken to be a δ-correlated white-noise process of zero mean satisfying

$$\langle \xi_i(t_1)\xi_j(t_2)\rangle = \delta_{ij}\delta(t_1 - t_2)\,; \tag{13}$$

this assumption greatly simplifies the calculations in the sequel. The discretized induction operator has the form

$$\boldsymbol{A} = \begin{pmatrix} -ikU_z + (1/R_m)\boldsymbol{L}_r & 0 \\ ikr\,d\Omega/dr & -ikU_z + (1/R_m)\boldsymbol{L}_\theta \end{pmatrix}, \tag{14}$$

where $\boldsymbol{L}_r$ is the discretized diffusion operator of equation (10), in which the appropriate boundary conditions for $\hat{B}_r$ are applied. The operator $\boldsymbol{L}_\theta$ is also the discretized diffusion operator in which the appropriate boundary conditions for $\hat{B}_\theta$ are imposed. The boundary conditions for these two fields are different.

A conducting inner boundary at $r = r_0$ requires that

$$\hat{B}_r(r_0) = 0\,, \quad \left.\frac{d(r\hat{B}_\theta)}{dr}\right|_{r_0} = 0\,. \tag{15}$$

If the domain extends to the symmetry axis, then regularity of the axisymmetric field components at the symmetry axis requires

$$\lim_{r\to 0} r\hat{B}_r = 0\,, \quad \lim_{r\to 0} r\hat{B}_\theta = 0\,; \tag{16}$$

we impose insulating boundary conditions at $r = 1$:

$$\hat{B}_\theta(1) = 0\,, \quad \left.\frac{d(r\hat{B}_r)}{dr}\right|_{r=1} = \frac{|k|K_0(|k|)}{K_0'(|k|)}\hat{B}_r(1)\,, \tag{17}$$

with K_0 the modified Bessel function and K_0' its derivative.

Magnetic field perturbations will be measured by their total magnetic field energy per unit volume, which is taken as the definition of the inner product for the column vector B:

$$\|B\|^2 = (B, B) \equiv \frac{1}{\mu_0(r_2^2 - r_1^2)}\int_{r_1}^{r_2} r\,dr(|\hat{B}_r|^2 + |\hat{B}_\theta|^2 + |\hat{B}_z|^2)\,. \tag{18}$$

We adopt a Riemann sum approximation for this integral; the inner product can then be written in matrix form in

[1] The number of discretization points n is selected so that convergence to the continuous operator is obtained. Convergence of the discretized induction equations is verified by doubling resolution. It was determined in this way that $O(R_m^{1/3})$ grid points are required.

terms of the column vector B as

$$\|B\|^2 = B^\dagger \boldsymbol{M} B , \tag{19}$$

where † denotes the Hermitian transpose and the magnetic energy metric matrix $\boldsymbol{M}$ is of the form

$$\boldsymbol{M} = \frac{2\delta}{\mu_0(r_2^2 - r_1^2)} \begin{pmatrix} r + (1/k^2)\boldsymbol{D}^\dagger \boldsymbol{D} & 0 \\ 0 & r \end{pmatrix} , \tag{20}$$

where μ_0 is the magnetic permeability of the medium and the spatial interval between two consecutive discretization points is denoted by δ. The discretized operator $\boldsymbol{D}$ arises from expressing the axial magnetic field component B_z in terms of the radial B_r and is given by

$$\boldsymbol{D} = \frac{1}{r^{1/2}} + r^{1/2} \frac{d}{dr} , \tag{21}$$

and $\boldsymbol{D}^\dagger$ denotes its adjoint in the inner product: $(\hat{B}_r, \hat{B}_r) = \int_{r_1}^{r_2} dr\, \hat{B}_r^* \hat{B}_r$ with the appropriate boundary conditions imposed on $\hat{B}_r$. The metric matrix $\boldsymbol{M}$ is manifestly positive definite and Hermitian.

In this inner product, the induction operator $\boldsymbol{A}$ in the presence of a mean velocity straining field is nonnormal, i.e., the induction operator does not commute with its adjoint, therefore $\boldsymbol{A}\boldsymbol{A}^\dagger \neq \boldsymbol{A}^\dagger \boldsymbol{A}$, implying that the eigenvectors of $\boldsymbol{A}$ are not orthogonal in this inner product and perturbation growth, measured in this inner product, is possible even when all the eigenvalues of $\boldsymbol{A}$ decay.

The forced response of the magnetic field obtained from equation (12) is given by

$$B(t) = \int_0^t e^{\boldsymbol{A}(t-s)} \boldsymbol{F} \xi(s) ds . \tag{22}$$

The ensemble average magnetic field energy maintained at time t by the stochastic forcing can be calculated making use of the properties of the white-noise vector ξ (eq. [13]) as follows (we make use of the summation convention):

$$\begin{aligned} \langle \|B(t)\|^2 \rangle &= \langle B_i^*(t) M_{ij} B_j(t) \rangle \\ &= \left\langle \int_0^t \int_0^t ds\, ds'\, e_{ia}^{A^*(t-s)} F_{ab}^* \xi_b^*(s) M_{ij} e_{jc}^{A(t-s)} F_{cd} \xi_d(s') \right\rangle \\ &= F_{ba}^\dagger \left(\int_0^t ds\, e_{ai}^{A^\dagger(t-s)} M_{ij} e_{jc}^{A(t-s)} \right) F_{cb} \\ &= \text{trace}\, [\boldsymbol{F}^\dagger \boldsymbol{Q}(t) \boldsymbol{F}] , \end{aligned} \tag{23}$$

in which the Hermitian operator

$$\boldsymbol{Q}(t) \equiv \int_0^t e^{\boldsymbol{A}^\dagger(t-s)} \boldsymbol{M} e^{\boldsymbol{A}(t-s)} ds \tag{24}$$

has been defined. This operator serves to accumulate over time t the magnetic energy from the stochastic forcing; through equation (23) $\boldsymbol{Q}(t)$ transforms the specific magnetic field forcings, the columns of $\boldsymbol{F}$, into the stochastically maintained mean magnetic field energy. When $\boldsymbol{A}$ has decaying spectrum, $\boldsymbol{Q}(t)$ integrates a product of decaying exponentials, thus ensuring the existence as $t \to \infty$ of the steady state matrix $\boldsymbol{Q}^\infty$. In practice, it is convenient to obtain $\boldsymbol{Q}^\infty$ directly from the solution of the Lyapunov equation:

$$\boldsymbol{A}^\dagger \boldsymbol{Q}^\infty + \boldsymbol{Q}^\infty \boldsymbol{A} = -\boldsymbol{M} , \tag{25}$$

where $\boldsymbol{M}$ is the energy metric matrix of equation (20). This Lyapunov equation results directly from differentiating equation (24) to obtain

$$\frac{d\boldsymbol{Q}(t)}{dt} = \boldsymbol{M} + \boldsymbol{A}^\dagger \boldsymbol{Q}(t) + \boldsymbol{Q}(t) \boldsymbol{A} , \tag{26}$$

the fixed point of which is obtained when $\boldsymbol{Q}^\infty$ solves equation (25). Note that solving for $\boldsymbol{Q}^\infty$ from equation (25) is computationally advantageous compared with integrating equation (24).

The expression for the ensemble average magnetic energy of equation (23) reveals that for a set of unitary forcings ($\boldsymbol{F}\boldsymbol{F}^\dagger = \boldsymbol{I}$, i.e., all forcings are orthonormal in the domain) the maintained magnetic energy structure is independent of the specific set of forcing distributions as

$$\text{trace}\, [\boldsymbol{F}^\dagger \boldsymbol{Q}(t) \boldsymbol{F}] = \text{trace}\, [\boldsymbol{F}\boldsymbol{F}^\dagger \boldsymbol{Q}(t)] = \text{trace}\, [\boldsymbol{Q}(t)] . \tag{27}$$

This implies that if the magnetic field is forced by any complete unitary set of spatial structures, the maintained magnetic energy will be the same. In the sequel we choose a unitary set of forcings in order to characterize most transparently the spatial and temporal response inherent in the mean induction equation. If the set of forcing functions $\boldsymbol{F}$ is not unitary, then the mean magnetic energy depends on the specific forcing. Nevertheless, the dependence of the response on the forcings is weak for highly nonnormal operators (Farrell & Ioannou 1993c).

Note that the eigenfunctions f_i of the positive definite Hermitian matrix $\boldsymbol{Q}(t)$ render the bilinear form $f_i^\dagger \boldsymbol{Q}(t) f_i$ an extremum and naturally order the magnetic field forcings according to their contribution to the maintained energy at time t. Consequently, the eigenfunction of $\boldsymbol{Q}^\infty$ with the largest eigenvalue corresponds to the forcing structure that contributes most to the statistically steady ensemble magnetic field energy. A particular unitary forcing matrix $\boldsymbol{F}$ can be constructed consisting of the eigenfunctions of $\boldsymbol{Q}^\infty$ ordered in columns according to their decreasing eigenvalues, which orders them in contribution to the stochastically maintained magnetic energy. The forcings ordered in this way will be referred to as the stochastic optimals. Because the induction operator $\boldsymbol{A}$ in the presence of velocity strain is nonnormal, these stochastic optimals are distinct from the eigenfunctions of the induction operator.[2]

If the spectrum of $\boldsymbol{Q}^\infty$ falls off rapidly with mode number, then only the first few stochastic optimals maintain most of the statistically steady magnetic energy, and the field is insensitive to other aspects of the forcing so long as the forcing adequately excites these few dominant stochastic optimal spatial structures.

The unitary set of stochastic optimals, which are ordered in their contribution to the excitation of the ensemble mean magnetic field energy, should be contrasted with the unitary set of structures ordered according to the fraction of the maintained ensemble mean magnetic field energy that each explains. This unitary set of magnetic field structures

[2] Consider the case in which the metric is the identity, $\boldsymbol{M} = \boldsymbol{I}$; then, directly or conversely, if $\boldsymbol{A}$ is normal, $\boldsymbol{A}$ commutes with $\boldsymbol{A}^\dagger$ and consequently their eigenvectors are the same. In that case the eigenvectors of $\boldsymbol{A}$ and the eigenvectors of $e^{\boldsymbol{A}^\dagger t} e^{\boldsymbol{A}t}$ coincide, and from eq. (24) it follows that the eigenvectors of $\boldsymbol{A}$ and the eigenvectors of $\boldsymbol{Q}(t)$, which are the stochastic optimals, also coincide. The proof is easily extended to an arbitrary metric by transforming the variable in the induction equation to $\boldsymbol{M}^{1/2} B$.

ordered according to their individual role in explaining the total ensemble mean magnetic field energy will be referred to as the empirical orthogonal functions (EOFs) of the maintained magnetic field; these are identical to the Karhunen-Loéve decomposition of the mean field. To obtain the EOFs, we form the magnetic field energy covariance matrix:

$$C_{ij}(t) = \langle [\boldsymbol{M}^{1/2}B(t)]_i [\boldsymbol{M}^{1/2}B(t)]_j^* \rangle = \left[\boldsymbol{M}^{1/2} \left(\int_0^t e^{\boldsymbol{A}(t-s)} \boldsymbol{F}\boldsymbol{F}^\dagger e^{\boldsymbol{A}^\dagger (t-s)}\, ds \right) \boldsymbol{M}^{1/2} \right]_{ij}, \quad (28)$$

where we have proceeded as in equation (23) and made use of the Hermitian and positive definite properties of the energy metric matrix $\boldsymbol{M}$. Consider the matrix, $\boldsymbol{X}$, consisting of the eigenfunctions of this covariance matrix arranged in columns. The EOFs are the columns of the matrix $\boldsymbol{M}^{-1/2}\boldsymbol{X}$. Because the covariance matrix is Hermitian, the EOFs form an orthonormal set of magnetic field structures in the magnetic field energy inner product (eq. [19]). The eigenvalues of the magnetic field covariance matrix are the statistically steady magnetic field energy accounted for by their corresponding eigenfunctions. The EOFs are ordered in descending order of their eigenvalues. By construction, the trace of the covariance matrix is the ensemble mean magnetic energy.

If $\boldsymbol{A}$ has a decaying spectrum, the covariance matrix integrates a product of decaying exponentials and the existence of the steady state covariance matrix $\boldsymbol{C}^\infty$ is ensured. Differentiation of equation (28) shows that the covariance matrix solves the equation

$$\frac{d\boldsymbol{C}(t)}{dt} = \boldsymbol{M}^{1/2}(\boldsymbol{F}\boldsymbol{F}^\dagger + \boldsymbol{A}\boldsymbol{M}^{-1/2}\boldsymbol{C}(t)\boldsymbol{M}^{-1/2} + \boldsymbol{M}^{-1/2}\boldsymbol{C}(t)\boldsymbol{M}^{-1/2}\boldsymbol{A}^\dagger)\boldsymbol{M}^{1/2}, \quad (29)$$

so that in the limit $t \to \infty$, for a stable $\boldsymbol{A}$, the covariance matrix solves the companion Lyapunov equation to equation (25):

$$\boldsymbol{A}\boldsymbol{M}^{-1/2}\boldsymbol{C}^\infty\boldsymbol{M}^{-1/2} + \boldsymbol{M}^{-1/2}\boldsymbol{C}^\infty\boldsymbol{M}^{-1/2}\boldsymbol{A}^\dagger = -\boldsymbol{F}\boldsymbol{F}^\dagger, \quad (30)$$

from which $\boldsymbol{C}^\infty$ is easily obtained given the induction operator $\boldsymbol{A}$ and the forcing matrix $\boldsymbol{F}\boldsymbol{F}^\dagger$; when $\boldsymbol{F}$ is unitary, $\boldsymbol{C}^\infty$ depends only on the dynamical operator and the chosen metric. Knowing $\boldsymbol{C}^\infty$ allows calculation of the magnetic field structures into which the magnetic energy is concentrated, the EOFs, which are related to the eigenfunctions of $\boldsymbol{C}^\infty$ through multiplication by the matrix $\boldsymbol{M}^{-1/2}$. The eigenvalues of $\boldsymbol{C}^\infty$ determine the fraction of the statistically steady magnetic energy accounted for by the corresponding EOFs. The volume-averaged magnetic field energy $\langle \|B\|^2 \rangle = \text{trace}\,(\boldsymbol{C}^\infty)$ is the sum of these eigenvalues.

If $\boldsymbol{A}$ is normal, the forcing is unitary ($\boldsymbol{F}\boldsymbol{F}^\dagger = \boldsymbol{I}$), and the metric is the identity, then $\boldsymbol{A}$, $\boldsymbol{C}(t)$, and $\boldsymbol{Q}(t)$ commute and the stochastic optimals, the EOFs and the modes of the dynamical system coincide. For such systems, eigenanalysis of $\boldsymbol{A}$ suffices for understanding the stochastic dynamics of perturbations in the linear limit. In contrast, for nonnormal systems such as that arising in the magnetic field generation problem in the astrophysical context, the stochastic optimals, the EOFs, and the modes of the induction operator are all distinct, and nonnormal analysis methods are necessary to solve for the steady state statistics.

3.2. *Spectral Properties of the Induction Operator in a Helical Flow*

We have already seen that the diffusion operators in equation (14) differ only in the boundary conditions imposed on them. The operator $\boldsymbol{L}_r$ acts on the radial magnetic field, while the operator $\boldsymbol{L}_\theta$ acts on the azimuthal, and the boundary conditions satisfied by these two fields are different (cf. eq. [17]). In the finite-dimensional representation of $\boldsymbol{L}_r$ and $\boldsymbol{L}_\theta$, this difference in boundary conditions leads to matrices that differ only in the entries that operate on the function values in the vicinity of the insulating boundary $r = 1$. The near-equality of the operators $\boldsymbol{L}_r$ and $\boldsymbol{L}_\theta$ for axisymmetric perturbations, and the fact that in $\boldsymbol{A}$ (cf. eq. [14]) the B_r vector uncouples from the B_θ vector, result in eigenfunctions of both $-ikU_z + 1/R_m\boldsymbol{L}_r$ and $-ikU_z + 1/R_m\boldsymbol{L}_\theta$ with nearly the same eigenvalue giving rise to the possibility of resonant excitation of the azimuthal field by the radial field. Indeed, examination of the stable spectrum of the dynamical operator $\boldsymbol{A}$ reveals that in the presence of both differential rotation and axial shear there exists a set of eigenfunctions with nearly degenerate eigenvalues trapped in the inner region which have only the azimuthal field component.

To examine this near resonance of the induction equation, consider the following velocity distribution in the region $0 < r < 1$:

$$\Omega(r) = 2\left\{\Omega_0 + \frac{1-\Omega_0}{2}\left[1 + \tanh\left(\frac{r-r_0}{\delta}\right)\right]\right\} \times \left[1 - \tanh\left(\frac{r-r_1}{\delta}\right)\right], \quad (31)$$

$$U_z(r) = \delta\sqrt{\frac{e}{2}}\frac{d}{dr}\left\{\exp\left[-\frac{(r-r_c)^2}{\delta^2}\right]\right\}, \quad (32)$$

where e is the base of natural logarithms. For a flow contained in a cylinder with outer radius $r = 1$, we choose $\Omega_0 = 0.4$, $r_0 = 0.345$, $r_1 = 0.6$, $r_c = 0.545$, and $\delta = 0.05$ to obtain a strong region of differential rotation adjacent to the model core boundary at $r = 0.25$, and a second region of differential rotation near $r = 0.6$ which adjusts the angular

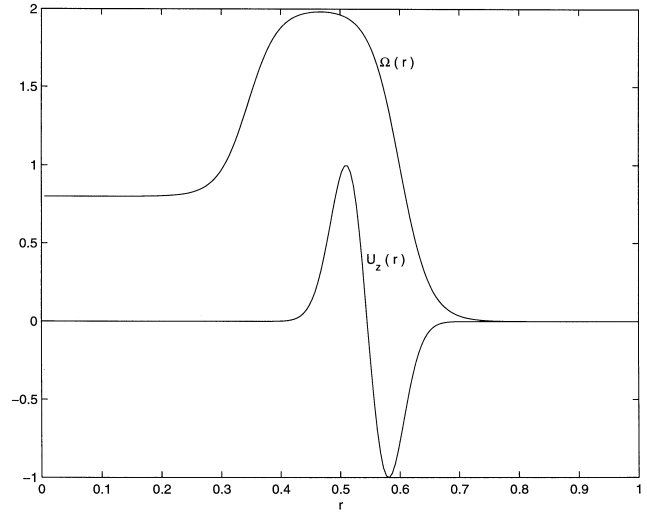

FIG. 1.—Angular velocity $\Omega(r)$ and axial velocity $U_z(r)$ as a function of radius of the helical flow as given in eqs. (31) and (32).

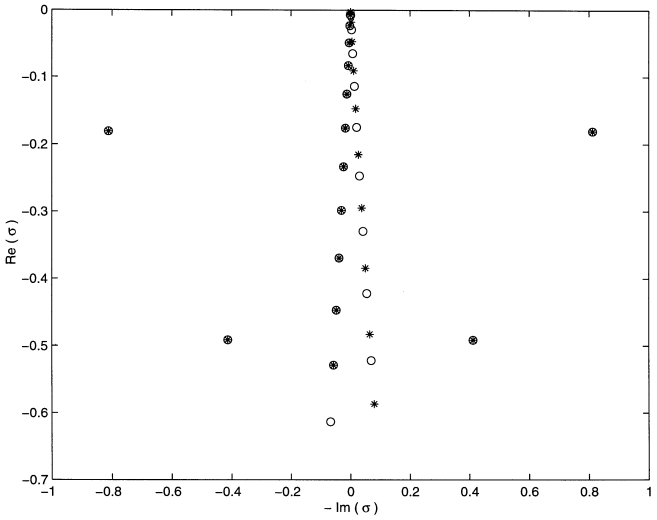

FIG. 2.—First 50 eigenvalues σ of the induction operator $\boldsymbol{A}$ for the flow given in eqs. (31) and (32) with azimuthal wavenumber $m = 0$ and axial wavenumber $k = -1$ at $R_m = 10^4$. The eigenvalues have been marked alternatively with circles and crosses in order to highlight the nearly resonant modes.

velocity to a zero value. Between these two regions of differential rotation we place a region of axial upwelling and downwelling modeling a meridional circulation adjacent to a core boundary. The angular velocity field (eq. [31]) and axial velocity field (eq. [32]) are shown in Figure 1.

The spectrum of the operator with velocity profile given by equations (31) and (32) for $R_m = 10^4$ and axial wavenumber $k = -1$ shown in Figure 2 reveals the existence of nearly resonant modes, the most important of which are the second and the third least damped pairs. The magnetic field components of the least damped eigenfunction, which is not nearly resonant, is seen in Figure 3 to be concentrated in the outer region near the insulating boundary.

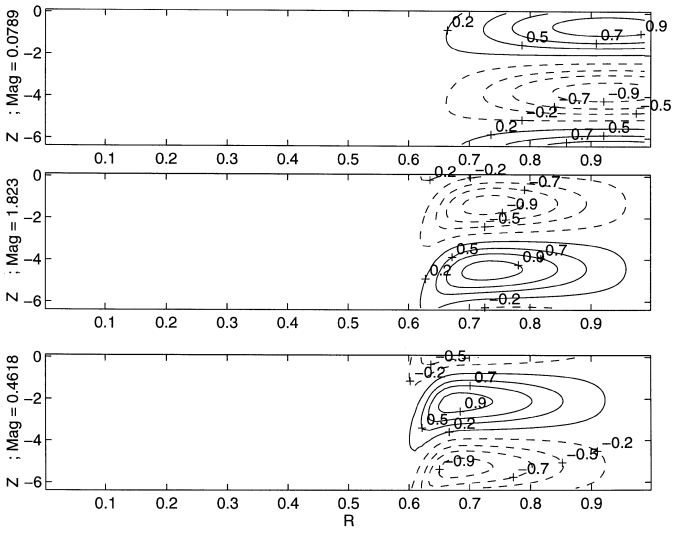

FIG. 3.—Radial magnetic field B_r (*top panel*), azimuthal magnetic field B_θ (*middle panel*), and axial magnetic field B_z (*bottom panel*) in the meridional plane (r, z) for the least stable mode for the flow shown in Fig. 1 at $R_m = 10^4$ with axisymmetric perturbations, azimuthal wavenumber $m = 0$, and axial wavenumber $k = -1$. The eigenvalue is $\sigma = -0.0027 - 0.0002i$. The magnetic field satisfies boundary conditions appropriate for regularity at $r = 0$ and an insulating outer wall. The maximum value of the corresponding field components is indicated in the ordinate label of each panel.

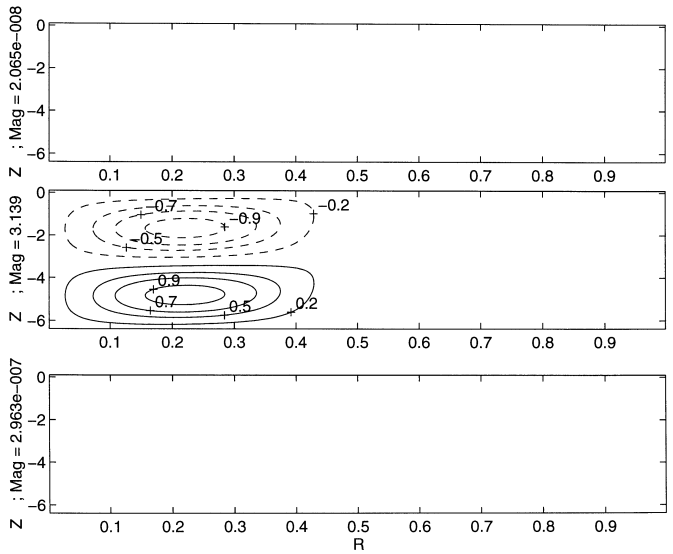

FIG. 4.—Radial magnetic field B_r (*top panel*), azimuthal magnetic field B_θ (*middle panel*), and axial magnetic field B_z (*bottom panel*) in the meridional plane for the first nearly resonant mode for the flow shown in Fig. 1 at $R_m = 10^4$ with axisymmetric perturbations, azimuthal wavenumber $m = 0$, and axial wavenumber $k = -1$. The eigenvalue is $\sigma = 0.0071 + 0.0006i$. The magnetic field satisfies boundary conditions appropriate for regularity at $r = 0$ and an insulating outer wall. The maximum value of the corresponding field components is indicated in the ordinate label of each panel.

Because the axial velocity is nearly zero in the outer region, the frequency of the mode is very small. As expected, the nearly resonant modes are concentrated near the symmetry axis where the $\boldsymbol{L}_r$ and $\boldsymbol{L}_\theta$ operators have the same boundary conditions. The structure of the field of the nearly resonant second and third eigenfunction (with approximately $\sigma = -0.0071 + 0.0006i$) in the same graph shown in Figure 4 reveals the coincidence of the eigenfunctions. As expected, the nearly resonant eigenfunctions involve only the azimuthal field which is concentrated near the symmetry but extends also into the region with differential rotation.

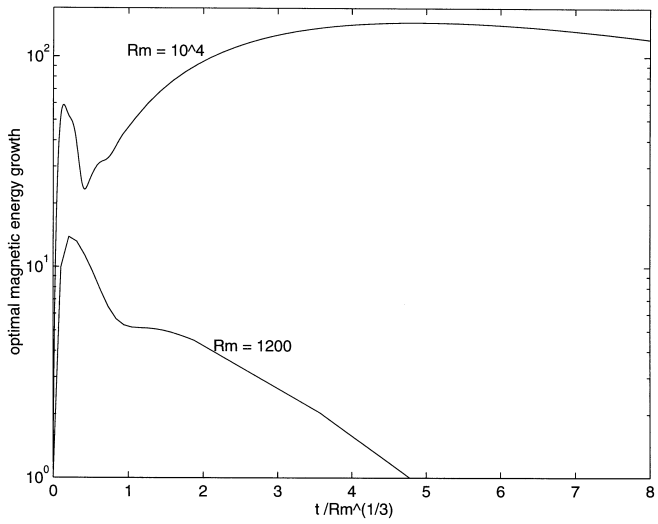

FIG. 5.—Optimal magnetic energy growth as a function of time scaled by $R_m^{1/3}$ for axisymmetric perturbations with axial wavenumber $k = -1$ for $R_m = 1200$ and 10^4. The flow is shown in Fig. 1. Note the secondary growth indicative of resonance.

The existence of nearly resonant eigenfunctions associated with a core azimuthal field gives the inner region particular dynamical significance. The presence of poloidal field in the vicinity of the inner region robustly excites growth of toroidal field in this region. Figure 5 shows the maximum energy attained by any initial perturbation of unit magnetic energy as a function of time. This is found by evaluating the square of the energy norm of the propagator of the induction operator (eq. [14]) i.e., $\| e^{\mathcal{A}^\dagger t} M e^{\mathcal{A}t} \|$ (for details see Farrell & Ioannou 1998). In the absence of resonance, the field decays after an initial energy growth leading to peak field energies of $O(R_m^{2/3})$ at a time of $O(R_m^{1/3})$, implying that stochastic forcing of the induction equation will produce ensemble mean magnetic energy of $O(R_m)$. By contrast, the resonant behaviour in Figure 5 shows that this initial energy peak is followed by persistent growth, which we shall see in the next section produces a pronounced increase in the forced response.

Resonant eigenfunctions can be strongly excited by fields in the core boundary region. In connection with field organization in stars, the radiatively dominated core is properly located below the convection zone and this boundary region has been implicated in supporting such fields (Layzer, Rossner, & Doyle 1979; Parker 1987).

4. AXISYMMETRIC RESPONSE OF THE INDUCTION EQUATION TO STOCHASTIC NOISE

4.1. *Organization of the Stochastically Maintained Magnetic Field*

Consider the statistically steady response to white-noise forcing of the induction equation with constant large-scale velocity field. For a normal dynamical system with decaying spectrum the energy maintained by stochastic forcing is proportional to the sum over the inverses of the decay rates of the modes, while the transient growth process in nonnormal dynamical systems such as the induction equation leads to ensemble energy levels that can be orders of magnitude greater. For example, if the induction equation matrix $\boldsymbol{A}$ is nearly defective,[3] indicative of a highly nonnormal system, then the maintained ensemble mean magnetic field energy can become especially large with the resulting resonant increase in energy scaling inversely as the cube of the decay rate of the resonant mode rather than inversely with the first power as for a normal system. If, as is often the case, the modal decay rates are proportional to R_m^{-1} then the mean magnetic field energy maintained increases in the presence of this resonance for large Reynolds number approximately as R_m^3, anticipating that the growth of the resonant modes dominates the magnetic energy.

The evolution of an initial magnetic field perturbation typically comprises a phase in which the field changes structurally and intensifies linearly in time due to stretching followed by a diffusive phase in which the field decays, eventually assuming the fixed structure of the least stable mode (cf. Farrell & Ioannou 1998). Consequently, the magnetic field structure that accounts for most of the mean field energy when the induction equation is stochastically forced will not be that of the least damped mode but rather a structure representing the mean over the growth-and-decay cycle of all excited perturbations. These mean structures are the EOFs which are found by eigenanalysis of the statistically steady covariance matrix $\boldsymbol{C}^\infty$ obtained from the dynamical operator through solution of the Lyapunov equation (eq. [30]). The eigenvalues of the positive definite Hermitian covariance matrix $\boldsymbol{C}^\infty$ can be ordered, and their corresponding orthogonal eigenfunctions order the functions (EOFs) according to their contribution to the mean field magnetic energy. The magnetic field associated with the first EOF, accounting for 87% of the mean magnetic energy, is shown in Figure 6*a*. This first EOF is distinct

[3] Defective matrices are those with linearly dependent corresponding eigenfunctions. This can happen only if the matrix is nonnormal. Normal matrices may have degenerate eigenvalues, but their eigenfunctions span the space.

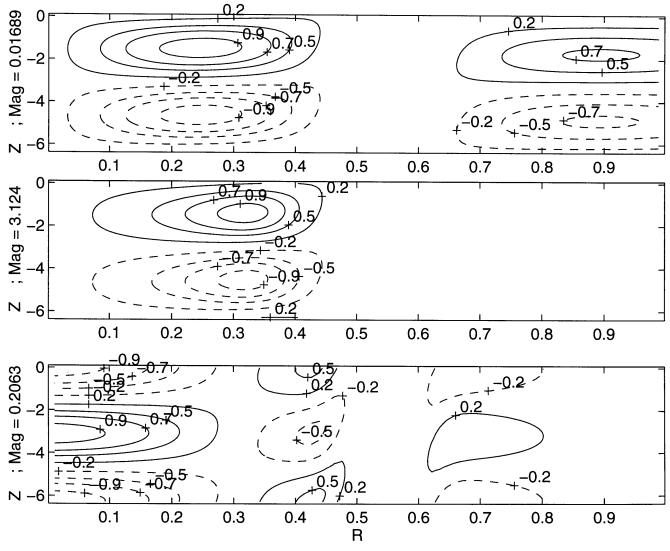

FIG. 6*a*

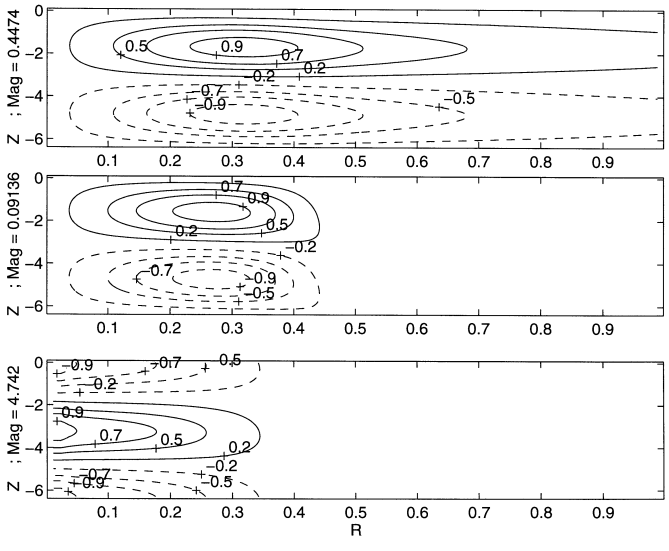

FIG. 6*b*

FIG. 6.—(*a*) Radial magnetic field B_r (*top panel*), azimuthal magnetic field B_θ (*middle panel*), and axial magnetic field B_z (*bottom panel*) in the meridional (r, z)-plane for the first axisymmetric EOF at Reynolds number $R_m = 10^4$ that accounts for 87% of the mean magnetic energy. The azimuthal wavenumber is $m = 0$, and the axial wavenumber is $k = -1$. The flow is shown in Fig. 1. The maximum value of the corresponding field components is indicated in the ordinate of each panel. (*b*) As in (*a*), but for the fields associated with the first stochastic optimal at $R_m = 10^4$, which when forced produces 90% of the ensemble mean magnetic field energy.

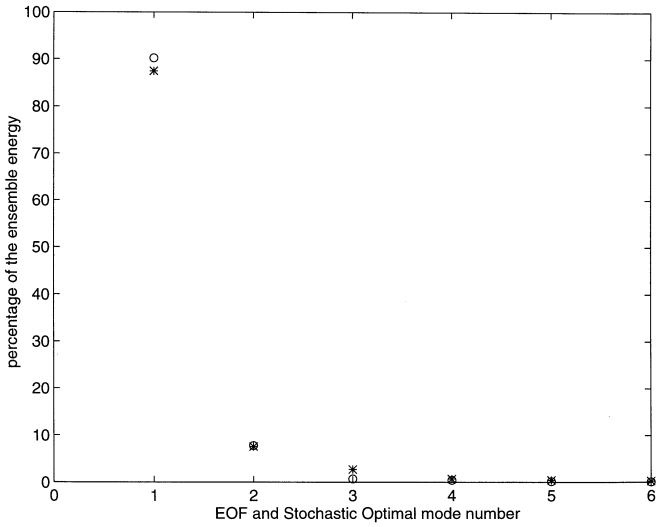

FIG. 7.—*Asterisks*: Percentage ensemble mean magnetic field energy accounted for by the first six empirical orthogonal functions (EOFs) of the magnetic field covariance ordered according to their contribution to the ensemble mean. *Circles*: Percentage ensemble mean magnetic field energy produced by the first six stochastic optimals ordered according to the ensemble mean energy each is responsible for producing. The example treats the stochastically forced axisymmetric field with azimuthal wavenumber $m = 0$ and axial wavenumber $k = -1$ at $R_m = 10^4$ for the flow shown in Fig. 1. Note that 99% of the ensemble mean energy is accounted for by the first three EOFs, and 99% of the ensemble mean energy is produced if the magnetic field forcing is restricted to the first three stochastic optimals.

from the least damped mode (cf. Fig. 3) due to the nonnormality of the dynamics, and specifically to the resonance between the toroidal and poloidal fields in the vicinity of the inner cylinder.

The first stochastic optimal, obtained by eigenanalysis of the matrix $\boldsymbol{Q}$ in equation (25), is the magnetic field forcing structure that maintains the largest magnetic field energy. It is responsible for producing 90% of the total magnetic field energy when all the ordered stochastic optimals are equally forced. This implies that the details of the stochastic forcing are not likely to be important provided that the stochastic forcing projects on the first stochastic optimal. The components of the magnetic field associated with the first stochastic optimal are shown in Figure 6*b*.

In Figure 7 the percentage of ensemble mean magnetic energy accounted for by the first EOFs and that forced by the first stochastic optimals are shown. Note that at $R_m = 10^4$ the mean magnetic field energy is explained by the first three EOFs and produced almost completely by the first three stochastic optimals. This indicates that the magnetic field energy can be described almost completely by the fields of the first three EOFs and produced by magnetic field forcing concentrated in the first three stochastic optimals. Concentration of the magnetic energy on the first EOFs demonstrates the process of organization of the large-scale field arising from the nonnormal growth processes.

4.2. *Temporal Variation of the Stochastically Maintained Magnetic Field*

The area average of the axial magnetic field, denoted $[B_z]$, over the conducting region at a given axial level is taken as a convenient proxy for the axisymmetric dipole moment, which has no exact counterpart in cylindrical coordinates. A time series of $[B_z]$ for the induction equation

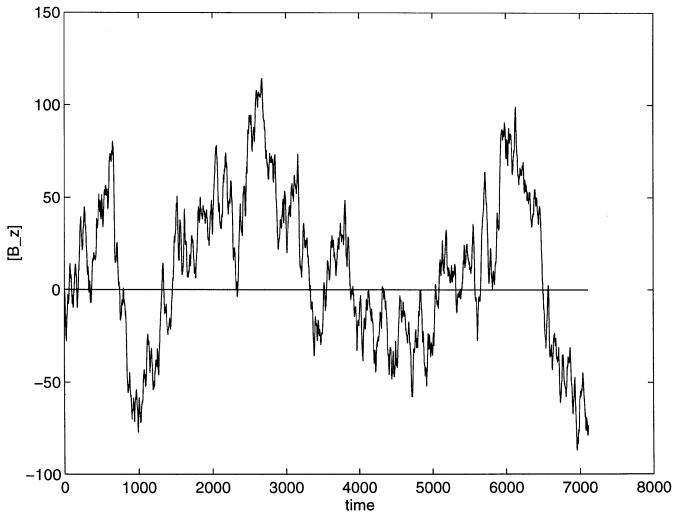

FIG. 8.—Time variation of the area-averaged axial magnetic field over the conducting region $[B_z]$ for axisymmetric perturbations with $k = -1$ at $R_m = 10^4$. The flow is shown in Fig. 1. The stochastic noise driving the induction equation is red with correlation time of 10 nondimensional units.

with insulating outer boundary and with red-noise forcing having correlation time 10 advective time units is shown in Figure 8. The response of the induction equation to stochastic forcing is aperiodic, but reversals typically occur separated by approximately 1000 nondimensional units. That the period between reversals greatly exceeds the advective timescale is due to the frequency response of the operator, which exhibits a very sharp peak near zero frequency as seen in Figure 9, which shows the power spectrum of the magnetic energy (the method used to obtain the power spectrum is described in the Appendix). The lower curve in the same figure shows the power spectrum of the ensemble mean magnetic field energy that results from exciting a normal operator with the same eigenvalues as the nonnormal induction operator that gave rise to the upper

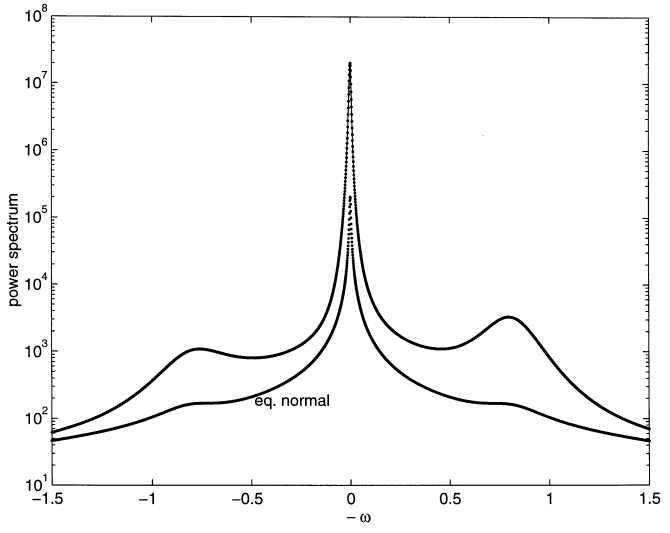

FIG. 9.—Power spectrum of magnetic field energy as a function of nondimensional angular frequency ω produced by stochastic forcing of the induction equation for the flow shown in Fig. 1 with azimuthal wavenumber $m = 0$ and axial wavenumber $k = -1$, and $R_m = 10^4$. Also shown (*lower curve*) is the equivalent normal response. Note that the response of the nonnormal induction operator is larger and of a different shape than that of the equivalent normal operator.

curve. Note that nonnormality leads to greater values of the energy power spectrum at all frequencies.

The nonnormal growth process can highly amplify selected modes of the system, consequently, if these modes are oscillatory and have decay rates that are long compared to their period, it is expected that the response will be nearly periodic. Such an example can be easily obtained. Consider the helical flow treated in Farrell & Ioannou (1998) which is confined between a conductor at $r = 0.5$ and an insulator at $r = 1$ with angular velocity $\Omega = e^{-r^2}$ and axial velocity equal to the angular velocity, and no radial velocity (the induction operator for this flow is not defective). A time series of $[B_z]$ for this case with insulating upper boundary is shown in Figure 10. The response is almost periodic with period approximately 15 advective time units consistent with the frequency of the second least damped mode, which is the only mode with appreciable $[B_z]$. This mode is effectively excited by stochastic forcing, as seen in Figure 11, where the power spectrum of the magnetic field energy is shown. The prominent peak at nondimensional frequency near -0.4 corresponds to the second least damped mode. The lower curve in the same figure shows the power spectrum of the ensemble mean magnetic energy that results from exciting a normal operator with the same eigenvalues. Note again that nonnormality leads to higher values of the power spectrum at all frequencies and especially higher response of the second least damped mode.

The examples treated were chosen to show that both nearly periodic and aperiodic responses may result from stochastic excitation.

4.3. *Energetics of the Stochastically Maintained Magnetic Field*

We have outlined a model for mean field maintenance in which nonmodal magnetic field growth sustains the large-scale ensemble mean magnetic field energy in response to stochastic forcing arising from the unresolved scales. One expects in such a system that the magnetic energy produced by stretching of the large-scale magnetic field by the large-scale velocity field would exceed the energy injected by the stochastic forcing, so that the primary energetic balance in the mean equation is between the nonmodal growth and diffusive dissipation, with the stochastic forcing assuming a catalytic role. This is not a logical necessity, however, as one may imagine energetics dominated by the unresolved scales with the mean induction operator acting simply to determine the mean field response to this forcing, as would occur for instance in the case of a stochastically forced normal system such as equation (4) in the absence of large-scale velocity and with the right-hand side of the equation replaced by a stochastic forcing term. Nevertheless, we expect that the resolved scale dynamics are energetically dominant and calculate the energetics of the stochastically forced induction equation.

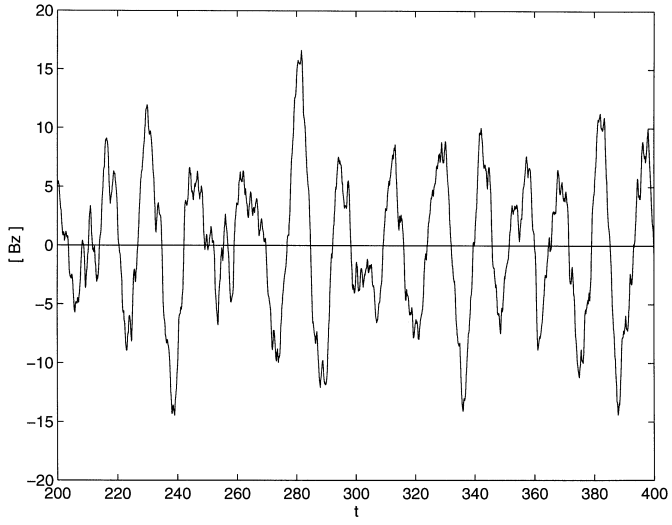

FIG. 10.—Axial field at fixed z averaged over the conducting region for axisymmetric perturbations with azimuthal wavenumber $m = 0$ and axial wavenumber $k = -1$ and $R_m = 10^4$. Magnetic field reversals are seen to occur with approximately 15 time unit period. The flow is $\Omega = U_z = e^{-r^2}$.

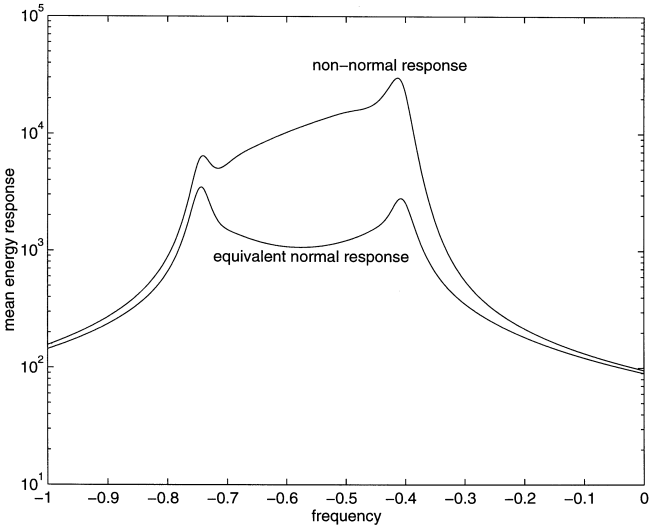

FIG. 11.—Power spectrum of magnetic field with azimuthal and axial wavenumbers $m = 0$ and $k = -1$, and $R_m = 10^4$ for the model problem with flow $\Omega = U_z = e^{-r^2}$. Also shown (*lower curve*) is the equivalent normal response. The prominent peak in the nonnormal response near nondimensional frequency -0.4 corresponds to the 15 advective time-unit period in the axial field seen in Fig. 10.

The energy is proportional to $\int_V \overline{\boldsymbol{B}}^2\, dV$ and an energy equation is obtained by multiplying equation (4) by $\overline{\boldsymbol{B}}$ and integrating over the fluid volume. If a statistical steady state is obtained, we have the following balance among the average rate of magnetic energy production by the deformation velocity field acting on the magnetic field (A), the average rate of stochastic input of magnetic energy (B), and the average rate of dissipation (C):

$$\underset{A}{\left\langle \int_V \overline{\boldsymbol{B}} \cdot (\bar{\boldsymbol{v}} \cdot \nabla)\overline{\boldsymbol{B}}\, dV \right\rangle} + \underset{B}{\left\langle \int_V \overline{\boldsymbol{B}} \cdot \boldsymbol{f}\, dV \right\rangle} = \underset{C}{\frac{1}{R_m} \left\langle \int_V (\nabla \wedge \overline{\boldsymbol{B}})^2\, dV \right\rangle}. \quad (33)$$

With the *Ansatz* of equation (13) all terms in equation (33) can be estimated directly from the covariance matrix $\boldsymbol{C}^{\infty}$.[4]

[4] For example, if we know the covariance of a field G, i.e., $C^G_{ij} = \langle G_i G_j^* \rangle$, then we can immediately calculate the covariance of any field that is a linear transformation of G, i.e., of $W = \boldsymbol{T}G$. Clearly $\boldsymbol{C}^W = \boldsymbol{T}\boldsymbol{C}^G\boldsymbol{T}^\dagger$.

At this point, we restrict the spatial scales of the forcing $\boldsymbol{f}$, which in a resolved discrete formulation corresponds to restricting the rank of $\boldsymbol{F}$. We retain m magnetic field forcings, which reduces the rank of the forcing matrix $\boldsymbol{F}$ from its full rank $2n$ to $m < 2n$. We assume this restriction because the relative magnitude of the terms in the energy equation (33) depends on the rank of the forcing matrix $\boldsymbol{F}$ because the stochastic input (B) is proportional to the number of degrees of freedom excited. It can be shown that the stochastic input per unit volume is

$$\left\langle \frac{1}{V} \int_V \overline{\boldsymbol{B}} \cdot \boldsymbol{f} dV \right\rangle \propto \text{trace } (\boldsymbol{F}^\dagger \boldsymbol{M} \boldsymbol{F} + \boldsymbol{F} \boldsymbol{M} \boldsymbol{F}^\dagger) , \qquad (34)$$

where the discrete representation of the stochastic forcing in equation (12) has been assumed. When each of the forcings (the columns of $\boldsymbol{F}$) is of unit magnitude and orthogonal in the $\boldsymbol{M}$ inner product, then the stochastic input increases in proportion to the number of degrees of freedom excited by the forcing matrix $\boldsymbol{F}$, while the ensemble mean magnetic field energy and the rate of magnetic energy production (A) increases most rapidly for the forcings that span the first few stochastic optimals, and as more forcings are added it converges to a finite value. Consequently, as the rank of the matrix increases, the ratio A/B decreases.

To assess the energetics we take a sequence of forcing matrices $\boldsymbol{F}_m$ each with columns the first m stochastic optimals obtained previously for the flow shown in Figure 1 ordered according to their contribution to the ensemble mean magnetic field energy. In Figure 12, the average rate of magnetic energy production for unit stochastic input is plotted as a function of the rank m of $\boldsymbol{F}_m$ for $R_m = 10^2$, 10^3, and 10^4. It is evident that the production term dominates the energetics provided only that the forcing is sufficiently limited in the basis of the stochastic optimals, which corresponds to limiting the excitation of highly damped small scales. Under these circumstances, the major energy source for the maintenance of the magnetic field is the kinetic energy of the mean velocity field.

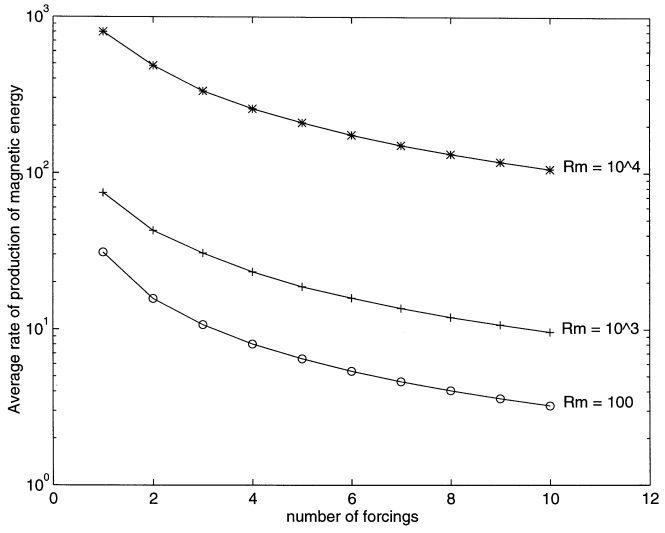

FIG. 12.—Rate of production of magnetic energy by the mean flow shown in Fig. 1 normalized by the stochastic input as a function of the number of stochastic optimals included in the forcing matrix $\boldsymbol{F}$. The stochastic optimals are ordered in descending order according to their contribution to forcing the maintained ensemble mean magnetic field energy. The average rate of production exceeds the stochastic input when it has a value greater than unity. The cases of $R_m = 10^2$, 10^3, and 10^4 are shown for the model problem. The azimuthal wavenumber is $m = 0$, and the axial wavenumber is $k = -1$.

5. DISCUSSION AND CONCLUSIONS

A major component of the theoretical basis for understanding amplification and organization of large-scale magnetic fields is the kinematic dynamo problem in which a velocity field is specified in a conducting fluid and the induction equation is solved to determine whether an initially small perturbation magnetic field grows. Traditionally, this problem has been studied by using the method of normal modes. The method of normal modes as it is usually applied seeks exponentially growing solutions to autonomous perturbation dynamical operators arising from linearization about a stationary mean state of a nonlinear dynamical system. In the case of the kinematic dynamo, however, the induction equation is explicitly linear in the magnetic field and if the Lorentz force can be ignored in the dynamical equation for the motion of the fluid, then the stability properties of the induction equation should determine the field growth and organization.

Stochastic excitation of the induction equation allows a model for the maintenance of large-scale mean fields to be constructed in which transient growth of perturbation magnetic field is primarily responsible for sustaining the field against diffusive damping. The stochastic forcing term can arise from two fundamentally different sources. If it arises from processes internal to the magnetohydrodynamics, then it constitutes a forcing of the resolved scales by the unresolved scales. However, the more general formulation of the forcing we have used allows also modeling a statistical steady state in which the primary forcing is produced by processes external to the magnetohydrodynamics itself. The structure and magnitude of the forcing may be specified by appeal to either theory or observation, but to be effective it must project on the restrictive subspace of structures the forcing of which results in the dominant contribution to accumulating the field energy, these being the stochastic optimals. The physical importance of including a stochastic parameterization of the fluctuating term arising from unresolved scales in the induction equation has been previously recognized, but perceived analytic difficulties in specifying the forcing with sufficient accuracy were thought to preclude implementation of this idea (Hoyng 1988). However, this objection is based on analysis of essentially normal model systems such as the α^2 dynamo,[5] in which the very great amplification of a small subset of modes, which we have seen in our example of the helical dynamo, does not occur. In highly nonnormal systems—such as the induction equation in strong shear—this extreme amplification of a restricted subspace of perturbations greatly simplifies the problem of parameterizing the forcing: the form of the forcing matters little so long as it projects on the highly growing subspace. The ensemble mean field energy is found to be concentrated in very few structures which demonstrate the inherent organization of the large-scale field. These dominant structures are dictated by the flow and not by the specific forcing.

[5] The α^2 dynamo example treated by Hoyng (1988) is slightly nonnormal, but the nonnormality stems only from the insulating boundary conditions at the surface of the conducting fluid and leads to a physically inconsequential modification of the modal dynamics as discussed by Hoyng (1988).

Alternatively, the right-hand side of equation (4) may be interpreted as arising from processes not directly involved in the magnetohydrodynamics, such as injection of turbulence into galaxies by massive stars and supernovae (McCray & Kafatos 1987; Minter & Spangler 1996) and small-scale turbulent convection in the case of stellar magnetic fields. The stochastic analysis described here is particularly suited to these cases in that it provides a theory for the structure and variability of the large-scale magnetic fields (EOFs) as well as information on which structures are the important components of the magnetic field forcing (stochastic optimals).

Direct numerical simulation and improved observations of stellar and galactic fields may soon provide a test for physically based conceptual models such as that presented here.

We thank Peter Hoyng for his helpful comments. This work was supported in part by NSF ATM-96132362.

APPENDIX A

POWER SPECTRUM ARISING FROM THE STOCHASTICALLY FORCED INDUCTION EQUATION

Asymptotically stable nonnormal dynamical systems exhibiting large transient response to impulsive forcing also exhibit enhanced asymptotic response to stochastic forcing. The response at a given frequency of a normal dynamical system is well known to depend on the proximity of the specified frequency to the resonant frequencies of the system (Hoyng & Schutgens 1995). In nonnormal dynamical systems the response additionally depends on the nonnormality of the operator, which can lead to a response orders of magnitude higher than that expected from normal resonance and additionally to a maximum of response not necessarily at the frequency of the least damped mode (Farrell & Ioannou 1994).

Consider the forced induction equation (12) with asymptotically stable induction operator $\boldsymbol{A}$:

$$\frac{dB}{dt} = \boldsymbol{A}B + \boldsymbol{F}\xi(t) \; . \tag{A1}$$

With the aid of the Fourier transform pair,

$$B(t) = \int_{-\infty}^{\infty} \hat{B}(\omega) e^{i\omega t} \, d\omega \; , \tag{A2}$$

$$\hat{B}(\omega) = \frac{1}{2\pi} \int_{-\infty}^{\infty} B(t) e^{-i\omega t} \, dt \; , \tag{A3}$$

the magnetic field response at frequency ω can be expressed as

$$\hat{B}(\omega) = \boldsymbol{R}(\omega)\boldsymbol{F}\hat{\xi}(\omega) \; , \tag{A4}$$

in terms of the resolvent

$$\boldsymbol{R}(\omega) = (i\omega\boldsymbol{I} - \boldsymbol{A})^{-1} \; , \tag{A5}$$

where $\boldsymbol{I}$ is the identity.

When all frequencies are excited equally, as would be the case for uncorrelated white-noise forcing of unit variance, i.e.,

$$\langle \hat{\xi}_i(\omega_1) \hat{\xi}_j^*(\omega_2) \rangle = \frac{1}{2\pi} \delta_{ij} \delta(\omega_1 - \omega_2) \; , \tag{A6}$$

the response ensemble mean magnetic field energy is given by

$$\begin{aligned} \langle \|B\|^2 \rangle &= \left\langle \int_{-\infty}^{\infty} \int_{-\infty}^{\infty} d\omega \, d\omega' B_i^*(\omega') M_{ij} B_j(\omega) e^{i(\omega - \omega')t} \right\rangle \\ &= \frac{1}{2\pi} \int_{-\infty}^{\infty} d\omega \, F_{ba}^\dagger R_{ai}^\dagger(\omega) M_{ij} R_{jc}(\omega) F_{cb} \\ &= \frac{1}{2\pi} \int_{-\infty}^{\infty} d\omega \, P(\omega) \; , \end{aligned} \tag{A7}$$

with the magnetic energy power spectrum defined as

$$P(\omega) = \text{trace} \, (\boldsymbol{F}^\dagger \boldsymbol{R}^\dagger(\omega) \boldsymbol{M} \boldsymbol{R}(\omega) \boldsymbol{F}) \; . \tag{A8}$$

Note that for unitary forcing, $\boldsymbol{F}\boldsymbol{F}^\dagger = \boldsymbol{I}$, the power spectrum is independent of the forcing structures.

The eigenvalues of the resolvent $\boldsymbol{R}$ are $(i\omega - \lambda_i)^{-1}$, and it can be shown that

$$P(\omega) \geq \sum_{i=1}^{N} \frac{\text{trace} \, (\boldsymbol{M})}{|i\omega - \lambda_i|^2} \; , \tag{A9}$$

with equality only when $\boldsymbol{A}$ is normal (Ioannou 1995). This inequality has the important implication that the power spectrum produced by spatially uncorrelated white-noise forcing of the nonnormal induction equation nearly always exceeds the power spectrum obtained as a summation of the contributions from the poles of the resolvent, often as is appropriate for the case of a normal operator. In practice, for highly nonnormal systems the nonnormal response is orders of magnitude larger than the equivalent normal response of the operator given by the right-hand side of equation (A9). This can be seen in Figure 9 for the flow shown in Figure 1, which has a defective dynamical operator, and in Figure 11 for the model flow $\Omega = U_z = e^{-r^2}$, which does not have a defective operator. In both cases the equivalent normal response is shown along with the nonnormal response.

The area under the curve of the energy power spectrum is the maintained ensemble mean magnetic field energy. Because of the nonnormal growth, the spectrum is highly peaked, which implies a long decorrelation time. In nonnormal systems such as the induction equation, estimates of decorrelation times based on the decay rate of the least damped mode may grossly underestimate the true decorrelation time.

REFERENCES

Braginskii, S. I. 1965a, Soviet Phys.—JETP Lett., 20, 726
———. 1965b, Soviet Phys.—JETP Lett., 20, 1462
Butler, K. M., & Farrell, B. F. 1992, Phys. Fluids A, 4, 1637
Childress, S., & Gilbert, A. D. 1995, Stretch, Twist, Fold: The Fast Dynamo (New York: Springer)
Choudhuri, A. R. 1992, A&A, 253, 277
Cowling, T. G. 1934, MNRAS, 94, 39
Farrell, B. F. 1982, J. Atmos. Sci., 39, 1663
———. 1984, J. Atmos. Sci., 41, 668
Farrell, B. F. 1988, Phys. Fluids, 31, 2093
———. 1989, J. Atmos. Sci., 46, 1193
Farrell, B. F., & Ioannou, P. J. 1993a, Phys. Fluids A, 5, 1390
———. 1993b, Phys. Fluids A, 5, 2600
———. 1993c, J. Atmos. Sci., 50, 4044
———. 1994, Phys. Rev. Lett., 72, 1188
———. 1995, J. Atmos. Sci., 52, 1642
———. 1998, Theor. Comput. Fluid Dynamics, 11, 215
Gustavsson, L. H. 1991, J. Fluid Mech., 224, 241
Hoyng, P. 1987a, A&A, 171, 348
———. 1987b, A&A, 171, 357
———. 1988, ApJ, 332, 857
Hoyng, P. 1992, in The Sun: A Laboratory for Astrophysics, ed. J. T. Schmeltz & J. C. Brown (Dordrecht: Kluwer), 99
———. 1993, A&A, 272, 321
Hoyng, P., & Schutgens, N. A. J., 1995, A&A, 293, 777
Ioannou, P. J. 1995, J. Atmos. Sci., 52, 1155
Kelvin, Lord. 1887, Philos. Mag., 24, 188
Layzer, D., Rossner, R., & Doyle, H. T. 1979, ApJ, 229, 1126
McCray, R., & Kafatos, M. 1987, ApJ, 317, 190
Minter, A. H., & Spangler, S. R. 1996, ApJ, 458, 194
Moffatt, H. K. 1978, Magnetic Field Generation by Electrically Conducting Fluids (Cambridge: Cambridge Univ. Press)
Orr, W. Mc F. 1907, Proc. R. Irish Acad., 27, 9
Ossendrijver, A. J. H., Hoyng, P., & Schmitt, D. 1996, A&A, 313, 938
Parker, E. N. 1955, ApJ, 122, 293
———. 1987, Sol. Phys., 110, 11
Rand, R. J., & Kulkarni, S. R. 1989, ApJ, 343, 760
Reddy, S. C., & Henningson, D. S. 1993, J. Fluid Mech., 252, 209
Steenbeck, M., & Krause, F. 1966, Z. Naturforsch., 21a, 1285
Steenbeck, M., Krause, F., & Rädler, K.-H. 1966, Z. Naturforsch., 21a 396
Zweibel, E. G., & Heiles, C. 1997, Nature, 385, 131